Intra-annual density fluctuations (IADFs) in Pinus nigra (J. F. Arnold) at high-elevation in the central Apennines (Italy)

Intra-Annual Density Fluctuations (IADFs) in *Pinus nigra* (Arn.) at high-elevation in the central Apennines (Italy)

Alma Piermattei [1*], Filipe Campelo [2], Ulf Büntgen [1,3,4], Alan Crivellaro [1], Matteo Garbarino [5], Carlo Urbinati [6]

Affiliations:

[1] Department of Geography, University of Cambridge, Downing Place, CB2 3EN, Cambridge, United Kingdom

[2] CFE – Centre for Functional Ecology – Science for People & the Planet, Department of Life Sciences, University of Coimbra, 3000-456 Coimbra, Portugal

[3] Dendro Science, Swiss Federal Research Institute - WSL, Zürcherstrasse 111, 8903, Birmensdorf, Switzerland

[4] CzechGlobe, Global Change Research Institute CAS and Masaryk University, Kotlářská 2, 61137, Brno, Czech Republic.

[5] Department DISAFA, Università degli Studi di Torino, Largo Braccini 2, 10095 Grugliasco, Italy

[6] Department of Agricultural, Food and Environmental Sciences – D3A, Marche Polytechnic University, 60100, Ancona, Italy

* Corresponding author (Alma Piermattei): alma.piermattei@geog.cam.ac.uk

Keywords: European black pine, anthropogenic forest limit, pioneer vs planted pines, standardized IADFs, Weibull and Chapman functions

Abstract

Although wood anatomical features can provide yearly resolved climatic information at sub-seasonal resolution, the occurrence of Intra-Annual Density Fluctuations (IADFs) might be triggered by several abiotic factors under different ecological settings. Here, we use information on cambial age and tree-ring width to standardize the frequency of IADFs in European black pines from three different mountain slopes in the central Apennines (Italy). At each site, we sampled 15–30-year pioneer pines from above the forest limit, as well as 40–60-year planted pines at the much denser forest limit. Mainly restricted to the latewood of both pioneer and planted trees, the occurrence of IADFs reveals a significant positive relationship with cambial age and ring width. Although the standardized IADFs are well synchronized between the planted and pioneer pines, the frequency of IADFs was higher in pioneer pines than in planted one, but only for narrow rings. Increased temperature and decreased precipitation from July to August are characteristic for the years with the highest IADFs frequency. Our study underlines the values of IADFs to obtain a more nuanced understanding of the climatic drivers of wood formation at the intra-annual scale.

Introduction

Tree-ring records are among the most important and common annually resolved climate proxies (Sheppard 2010). As tree-ring widths are commonly used to infer climate annual variability, intra-ring wood anatomical traits, such as Intra-Annual Density Fluctuations (IADFs), resin canals density, and maximum wood density, can provide useful climate-growth information with a sub-seasonal resolution (De Luis et al. 2007; Esper et al. 2015; Björklund et al. 2017). However, the role of the numerous climatic factors affecting wood formation is not clearly understood at the intra-annual level (Olano et al. 2012). Within the growing season, environmental and climatic variations set the pace of cambial activity and cells development leading eventually to IADFs formation (e.g., Bogino et al. 2009; Battipaglia et al. 2016). The position of IADFs within tree rings (e.g., in earlywood or in latewood) is also determined by the timing of the triggering factor (Campelo et al. 2007). Therefore, the study of IADFs can help to detect the changes in cambial activity within the growing season (Campelo et al. 2007; Rozas et al. 2011; De Micco et al. 2014). However, the IADFs occurrence is not straightforward, since their formation is not only climate driven, but also influenced by other factors, such as slope-aspect, tree species, tree status, tree age, and tree-ring width (Vieira et al. 2009; Campelo et al. 2013; Klisz et al. 2016; Zalloni et al. 2016; Campelo et al. 2018).

Recently, new analytical methods have been developed to disentangle IADFs triggering factors. Novak et al. (2013) assessed the IADF climatic signal in *Pinus halepensis* in Spain applying a three-parameter Weibull function to remove

the effect of cambial age on IADFs frequency. Campelo et al. (2015) removed direct ring-width and indirect cambial-age effects from IADFs chronologies after standardizing with a Chapman function. Both methods removed the effect of predisposing factors (e.g., ring width and cambial age) in order to increase or add new signals to IADFs chronologies. For example, a negative effect of September temperature on IADF formation was detected only after removing the ring-width effect (Campelo et al. 2015).

In this study, we investigated tree-ring growth and IADFs occurrence on European black pine (*Pinus nigra* Arnold) growing at high altitude in three sites at the central Apennines, Italy. In addition, we proposed a revised method to remove the tree-ring width and age effects from IADFs chronologies using both a Chapman and Weibull function.

At each site, we sampled planted pines (PLP) at the upper closed forest border, and pioneer pines (PIP) occurring above the anthropogenic upper forest line. PLP were planted in the 1950s, whereas PIP naturally encroached 15–20 years later when the planted pines reached maturity and dispersed seeds (Piermattei et al. 2014; Vitali et al. 2017). Planted pines are older, located at lower altitude, and grow at a much higher tree density than pioneer pines that are mainly isolates. We tested the following two hypotheses: *i*) The IADFs frequency in pioneer pines is higher than in planted pines due to the more limiting growing conditions and to tree ages, and *ii*) the IADFs frequency is synchronized among the three sites for PIP and PLP, highlighting a common climatic driven.

Material and methods

Study Sites

The three sites are Mt. Vettore (VET), Mt. San Franco (SFR) and Mt. Ocre (OCR) in the central Apennines (Italy). They are located within the Sibillini Mts. National Park, Gran Sasso and Laga Mts. National Park, and Acquazzese Forest Natural Reserve respectively at a reciprocal distance of about 30 km (**Fig. 1**). We sampled at high elevation near and above the anthropogenic central Apennines treelines usually featuring beech forests on north- and pine plantations on south facing slopes. Sites differ in aspect, slope angle and altitude of the forest line (**Table 1, Fig. 1**). At all sites, we sampled PLP close the upper edge of the forest limit. At VET and SFR, we sampled PIP along the entire ecotonal area above the forest line; whereas at OCR we limited the area to an altitudinal transect 200 m wide extending to the mountain top due to the higher density of pine cohorts. At all sites PIP are randomly distributed between 1600 and 2100 m a.s.l. (Piermattei et al. 2016).

Tree-ring Data Analysis

Dendrochronological sampling took place between 2009 and 2014 collecting one basal increment core from each pioneer pine and two breast height cores from planted pines. All cores were mounted on wood supports and polished using sandpapers of a progressively finer grain (from 240 to 1000 grit) until tree-ring boundaries and cells were clearly visible under a binocular stereomicroscope. Tree-ring width was measured with the LINTAB device and TSAPWin software (Rinntech, Germany) to 0.01 mm precision. Cross-dating quality was checked visually and using COFECHA software (Holmes, 1983). Individual series were checked with a local master chronology and deleted from the dataset if Pearson's correlation coefficient was less than 0.4. For pioneer pines, only cores with more than 15 tree rings, without visible damage and showing the pith were selected. For planted pines, from each tree the core with the highest number of tree-rings was used, and the selection was random when both cores showed the pith. PLP and PIP tree-ring width series were detrended using a 20-years smoothing spline with 50% frequency cutoff, which isolated high-frequency variability using the R packages detrendeR (Campelo et al. 2012) and dplR (Bunn 2008). Autoregressive modelling was performed to remove the temporal autocorrelation. Finally, a biweight robust mean was computed to average the individual series and to produce standardized tree-ring width chronologies. For each PLP and PIP, mean chronology, the mean sensitivity (MS), the first-order autocorrelation (AC1), the inter-series correlation (Rbar) and the expressed population signals (EPS, Wigley et al. 1984) was computed. Mean width, MS and AC1 were calculated on raw data, while Rbar and EPS on indexed series. Spearman's correlation of PLP and PIP tree-ring width chronologies between and within sites was also calculated.

Intra-Annual Density Fluctuations

To detect the IADFs presence and type, a stereomicroscope up to a 25× magnification was used. IADFs were classified according to their positions within the tree ring in type E characterized by latewood-like cells within earlywood; type E+ with transition cells between earlywood and latewood; type L formed by earlywood-like cells within latewood, and type L+ showing earlywood-like cells between latewood and earlywood of the following tree ring (Campelo et al. 2007). Since the occurrence of IADFs in the earlywood (E and E+) was very low, only the frequency of IADFs in the latewood zone (L, L+ or both LL+) was used. Because their non-normal distribution, IADFs frequency cannot be used directly as a continuous variable in regression equations. Therefore, a binary dataset assigning the value 1 for presence or 0 for absence of IADFs in each tree ring of the series was built. There are different approaches to develop IADFs chronologies, correcting the bias introduced by changing sample depth over time (Osborn et al. 1997), by cambial age

(Novak et al. 2013), and by size (Campelo et al. 2015). To calculate the IADFs frequency through time with different sample depth, the method of Osborn et al. (1997) was applied. The adjusted IADFs frequency was calculated as follow:

$$f(\text{stabilized IADF frequency}) = F \times n^{\wedge 0.5}$$

where F is the ratio of N/n, N is the number of trees that showed an IADF type in a given year, and n is the total number of observed trees. However, to develop IADFs chronologies with the exclusion of age and the size effect, the method proposed by Campelo et al. (2015) was adapted. Tree rings were sorted based on their widths, and then ring width effect on IADFs occurrence was removed by fitting a Chapman or a Weibull function. The selection of the best function was determined using the Akaike's Information Criteria (AIC) that correspond to the lowest AIC Value (Akaike 1974). According to the Chapman function, the IADF frequency increases with tree-ring width up to a maximum value and afterwards reached a plateau, whereas the Weibull function decreases after reaching its maximum. This means that IADFs occurrence probability decreases for wider tree rings. Finally, the obtained IADF frequency indices were averaged into a chronology of IADFs. The resulting IADFs chronology are considered standardized and assumed to be independent from age and size. Spearman's correlation of PLP and PIP standardized IADFs chronologies between and within sites was also calculated.

Climatic data

Monthly data of mean, minimum and maximum air temperature (Tmean, Tmin and Tmax) and precipitation (Pre) were retrieved from the CRU TS V.4.0 database through the Climate Explorer application (http://climexp.knmi.nl). The gridded data were then corrected for the mean altitude value of each site, using the climate software package ClimateEU v.4.63 (http://tinyurl.com/ClimateEU, Hamann et al. 2013). To assess IADFs-climate relationships, Pearson's correlation analysis of climatic data with standardized IADFs chronologies for the common period 1984-2008 was applied. This time interval was determined based on sample replication more than four trees.

Results

Tree-ring chronologies

The sample depth at each site ranges from 17 to 29 trees. The mean age is 48 years for PLP, and 24 years for PIP (**Table 2**). PLP have high values of first-order autocorrelation (AC1). The mean tree-ring width of pioneer pines is lower than in planted ones, as well as for maximum width ranging from 1.25 to 7.5 mm in PIP, and from 4.30 to 10.6

mm for PLP (**Table 3**). PLP radial growth curves show a clear negative trend after 1970, whereas PIP shorter curves are relatively steady without evident age effect (**Fig. 2**). One of the largest PIP tree-ring widths is in 2003, followed by a narrow ring in 2004. Spearman's correlation of PLP and PIP chronologies are not always significant among and within sites (**Table S1**). PIP are higher correlated than PLP but only for OCR-SFR ($r = 0.56$, $p < 0.05$) and OCR-VET ($r = 0.46$, $p < 0.05$). Correlation coefficients in PLP range from 0.35 to 0.41 for all pairs. PIP chronologies are significant correlated ($p < 0.05$) with PLP only at VET ($r = 0.54$, $p < 0.05$) and SFR ($r = 0.43$, $p < 0.05$) sites.

IADFs frequencies and climatic signals

Results show consistency between stabilized IADFs frequency in planted and pioneer pines for each site with an increasing frequency in 1970-1980 for PLP and in 1995-2005 in PIP (**Fig. 3**). In PLP, the stabilized IADFs frequency declines during the last 10-20 years mainly at VET and OCR site, showing a left-skewed trend with a maximum peak in the juvenile phase.

The years with high-stabilized IADFs frequency are listed in **Table 4**. The averaged mean temperatures and precipitation for the years with the highest stabilized IADF frequency indicate a clear negative signal for July and August precipitation, respectively for planted and pioneer pines (**Fig. 4**). Mean temperatures signal is less pronounced even if their peaks coincide with the peaks of minimum precipitation.

Most of IADFs occurred in the latewood, and are mainly of L+ and L types. The frequency of IADFs of PIP and PLP considering the different sample depths and time interval for each site is depicted in **Table 5**. SFR shows the highest IADF frequency in PLP and PIP for the entire timespan and for the common interval (1984-2008) and at VET the PIP's IADF frequency is always higher than in PLP.

The relationship between standardized frequency and ring-width is described by exponential curves that tend to stabilize in all cases (Chapman function) except for VET pioneer and OCR planted (Weibull function) that decline after 4 mm (**Fig. 5**). PLP in general have a slightly higher frequency than PIP (between 0.4 and 0.55). Nonetheless, VET planted has the lowest frequency value (max 0.3). PIP frequency is higher for narrow rings than for PLP, and becomes steady with 2-3 mm of ring width (SFR and OCR) whereas PLP with 3-4 mm (VET and SFR) (**Fig. 5**).

The standardized IADFs chronologies by tree-ring width and age effect show high synchronicity over time within and between sites (**Fig. 6 A-C**). Spearman's correlation of planted and pioneer pines IADFs chronologies are always significant among and within sites (**Table S2**). Correlation coefficients in PLP range from 0.48 to 0.58 for all pairs. PIP IADFs chronologies are significant correlated ($p < 0.05$) with PLP at VET ($r = 0.48$, $p < 0.05$), SFR ($r = 0.67$, $p < 0.05$), and OCR ($r = 0.38$, $p < 0.05$) sites.

169 The IADFs-climate relationships do not show an overall pattern but some similarity within site, mainly in SFR (**Fig. 7**).
170 Correlations between standardized IADFs and averaging December (t-1) - January (t) precipitation is common at all
171 sites in PIP. However, the strongest correlations appear between standardized IADFs and temperatures with both
172 positive and negative effects at SFR and VET sites. In fact, a negative correlation is found in spring months (averaging
173 February and March (t)) in PIP, and a positive signal with July (t) temperatures in PLP.
174
175 **Discussion**

176 The dendroclimatic tree-ring width signal derived from planted pines growing in dense stands and from pioneer pines
177 too young for a robust dendroclimatic analysis, is complex and difficult to interpret. In our study, the combination of the
178 yearly resolved IADFs frequency and the type of analyses conducted enhanced the climatic signal. The 2003 heatwave
179 represents a clear pointer year in tree-ring width series, whereas frequency of stabilized and standardized IADFs
180 provided proof for a common pattern and a summer climatic signal that, however, must be discuss in respect to tree age
181 and ring width.

182 *Radial growth of pioneer and planted pines*

183 In the last 20–30 years, PLP reduced their ring widths, as opposed to PIP, which displayed a steady or even increasing
184 tree-ring width trend peaking in 2003, a year with a hot and dry summer throughout Europe (e.g. Luterbacher et al.
185 2004). The evidence of an enhanced ring width for PIP recorded in 2003 (Fig. 2), a growing season with high
186 temperatures and high June precipitation (Fig. S1) suggests that increasing temperatures associated with rainfalls could
187 favour tree-ring growth at the upper forest limit by extending the growing season. In fact, the 2003 growing season was
188 2%, 12% and 64% longer in subalpine, alpine and nival areas respectively, and induced and exceptional increase of
189 basal area in subalpine species in Europe (Jolly et al. 2005). Noteworthy, after the 2003 heatwave, both pioneer and
190 planted pines respond with an abrupt tree-ring width reduction probably caused by a dry summer in 2004 (Fig. S1). In
191 PLP, the drought effect lasted to 2005, the year with the narrowest ring width (Fig. S2). This can explain the high value
192 of first-order autocorrelation in tree-ring width, especially for PLP, indicating the lag effect of previous year on current
193 growth of black pine. Moreover, besides some differences in site features (e.g. aspect and slope), a common growth
194 pattern is revealed by high inter-series correlation coefficients (Rbar), and by a high cross-correlation *r*-values between
195 PIP and PLP site chronologies. The only exception is the north exposed site (OCR) probably due to different growing
196 conditions.
197

198 *IADFs characteristics and relationships with age and tree ring width*

199 Most of the IADFs are in the latewood, with the highest frequency in the south-west site. IADFs featured by earlywood-
200 like cells within latewood (L type), and earlywood-like cells between latewood and earlywood of the following tree ring
201 (L+ type, Campelo et al. 2007). The genus *Pinus* is prone to latewood IADFs production and their formation occurs
202 after a summer drought in early (L) or late (L+) autumn (e.g. Rigling et al. 2001; Masiokas and Villalba, 2004; Campelo
203 et al. 2007; Vieira et al. 2009; Battipaglia et al. 2010; De Luis et al. 2011; Rozas et al. 2011; Carvalho et al. 2015).
204 Previous studies on pine species of the Mediterranean basin proved that the most important factor linked to latewood
205 IADFs formation is autumn precipitation of the current growth year (e.g. Zalloni et al. 2016; Vieira et al. 2017).

206 Nonetheless, the central Apennines are not under the typical Mediterranean bioclimatic conditions. The three sampled
207 sites share a temperate oceanic macrobioclimate (sensu Rivas-Martinez and Rivas-Saenz 2009) with short drought
208 periods in July-August and precipitation peaks in early spring and autumn. The growing season at 1600 m elevation
209 extends from beginning of June to mid-late October. The transition from earlywood to latewood occurs usually in
210 August and most of the latewood cells are formed in September, and maturation and lignification processes are
211 completed in October (Piermattei et al. 2015). Few earlywood IADFs (type E, and E+) are found (e.g. 1973, 1974) and
212 only in PLP. Their formation usually follows a water deficit early in the growing season (e.g. Wimmer et al. 2000;
213 Campelo et al. 2007), a condition uncommon in the study areas where snowfalls can be abundant in late winter
214 (February and March) and occasionally extend to May and the beginning of June (De bellis et al. 2010).

215 Moreover, to investigate the effect of climate on IADFs frequency over time, we need to compensate the less (high)
216 probability to have IADFs in narrow (wide) tree-ring width (Rigling et al. 2001, 2002; Battipaglia et al. 2010; Campelo
217 et al. 2013; Novak et al. 2013), and that tree-ring widths commonly decrease with age. We expect higher IADFs
218 frequency in wider rings because more cells are under the differentiation phase for a longer period, which induced the
219 IADF formation once the triggering factor occurred (Campelo et al. 2015; Vieira et al. 2018). Other studies also found
220 more IADFs in younger trees than in older ones (e.g. Copenheaver et al. 2006; Vieira et al. 2009, 2010). Our results
221 confirmed the effect of age and tree-ring width on IADFs formation. In fact, besides the stabilized IADFs frequency is
222 highly synchronized, PLP showed an increase in IADFs frequency in the year 1970–1990 with a decline in the last
223 years that could be linked to ring width reduction, evident at VET and OCR sites. In narrow rings (< 2 mm), the higher
224 IADF frequencies occurred in PIP, whereas an increase of IADF frequency is expected in relatively wider rings (> 2
225 mm) as obtained by Zalloni et al. (2016), where IADFs frequency peaked in 3–5 mm wide tree rings and in 19–38 years
226 old trees.

In this study, we used both a Weibull and a Chapman function to standardize the IADFs frequency from age and tree-ring width (Novak et al. 2013; Campelo et al. 2015). Our combined method to standardize IADF frequency (with the two possible curves) enables to detect a decreasing IADF formation probability in wider rings using the Weibull curve as it happens in VET pioneer and OCR planted pines. IADFs are not formed if a wider ring can be formed when environmental conditions are favourable and stable throughout the entire growing season.

The frequency of standardized IADFs appeared synchronized within and between the study sites, suggesting a common driver of IADF formation. Accounting only for the years with the highest IADFs frequency a clear pattern appears: a combination of low precipitations and high mean temperatures in July and August caused the maximum IADFs occurrence respectively in PLP and PIP, likely induced by dry and hot summer conditions. However, considering the standardized IADFs-climate relationship in the common interval 1984-2008, this result is confirmed only in PLP. The positive correlation with July temperature is probably related to a water deficit particularly at VET and SFR, respectively south and south-west exposed. Our result is consistent with the study by Campelo et al. (2018) where IADFs are more frequent in south-facing slope trees, with a longer growing season. Instead, the weakness of the climatic sensitivity of standardized IADFs in pioneer pines might be due to a combination of precipitation, temperatures, and soil moisture, where microsite conditions play a fundamental role, highlighting a possible individual adaptation. In conclusion, with this study we want to promote the standardization method to highlight the climatic effect on IADFs chronologies.

Acknowledgements

We wish to thank the following institutions and people for providing sampling authorisation, logistic support, and field and laboratory assistance: Monti Sibillini National Park, Gran Sasso-Monti della Laga National Park, Sirente-Velino Regional Park, and Bruno Petriccione, Francesco Renzaglia, Valeria Gallucci, Emidia Santini, Luca Bagnara, Matteo Giove, Andrea Cola, Simone Cingolani, Marco Altieri, Alessandro Vitali, and Edoardo Piermattei. We would also like to thank Giada Centenaro for assistance in preparing figure 1. This research was partly funded by Marche Polytechnic University grants.

255 **References**

256 Adams HR, Barnard HR, Loomis AK (2014) Topography alters tree growth–climate relationships in a semi-arid
257 forested catchment. Ecosphere 5(11):1-16.

258 Akaike H (1974) A new look at the statistical model identification. IEEE Trans. Automat. Control AC-19, pp. 716–23

259 Battipaglia G, De Micco V, Brand WA, Linke P, Aronne G, Saurer M, Cherubini P (2010) Variations of vessel diameter
260 and d13Cin false rings of Arbutus unedo L. reflect different environmental conditions. New Phytol 188:1099–1112.

261 Battipaglia G, Campelo F, Vieira J, Grabner M, De Micco V, Nabais C, Cherubini P, Carrer M, Bräuning A, Čufar K,
262 Di Filippo A, García-González I, Koprowski M, Klisz M, Kirdyanov AV, Zafirov N, De Luis M (2016) Structure and
263 function of intra-annual density fluctuations: mind the gaps. Front. Plant Sci. 7:595.

264 Björklund J, Seftigen K, Schweingruber F, Fonti P, von Arx G, Bryukhanova MV, Cuny HE, Carrer M, Castagneri D,
265 Frank DC (2017) Cell size and wall dimensions drive distinct variability of earlywood and latewood density in Northern
266 Hemisphere conifers. New Phytologist 216:728–740.

267 Bogino SM and Bravo F (2009) Climate and intra-annual density fluctuations in *Pinus pinaster* subsp. *mesogeensis* in
268 Spanish woodlands. Can. J. For. Res. 39:1557–1565.

269 Bräuning A (1999) Dendroclimatological potential of drought-sensitive tree stands in southern Tibet for the
270 reconstruction of monsoonal activity. IAWA J 20:325–338.

271 Bunn A (2008) A dendrochronology program library in R (dplR). Dendrochronologia 26:115–124.

272 Campelo F, García-González I, Nabais C (2012) detrendeR – A Graphical User Interface to process and visualize tree-
273 ring data using R. Dendrochronologia 20:57-60.

274 Campelo F, Nabais C, Freitas H, Gutierrez E (2007) Climatic significance of tree-ring width and intra-annual density
275 fluctuations in *Pinus pinea* from a dry Mediterranean area in Portugal. Annals of Forest Science 64:229–238

276 Campelo F, Vieira J, Battipaglia G, De Luis M, Nabais C, Freitas H, Cherubini P (2015) Which matters most for the
277 formation of intra-annual density fluctuations in *Pinus pinaster*: age or size? Trees 29:237–245.

278 Campelo F, Vieira J, Nabais C (2013) Tree-ring growth and intra- annual density fluctuations of *Pinus pinaster*
279 responses to climate: does size matter? Trees 27:763–772.

Campelo F, Gutiérrez E, Ribas M, Sánchez-Salguero R, Nabais C, Camarero JJ (2018) The facultative bimodal growth pattern in *Quercus ilex* – A simple model to predict sub-seasonal and inter-annual growth. Dendrochronologia 49:77–88. doi:10.1016/j.dendro.2018.03.001.

Carvalho A, Nabais C, Vieira J, Rossi S, Campelo F (2015) Plastic Response of Tracheids in *Pinus pinaster* in a Water-Limited Environment: Adjusting Lumen Size instead of Wall Thickness. PLoS ONE 10(8): e0136305.

Copenheaver CA, Pokorski EA, Currie JE, Abrams MD (2006) Causation of false ring formation in *Pinus banksiana*: a comparison of age, canopy class, climate and growth rate. Forest Ecology and Management 236:348–355.

De Bellis A, Pavan V, Levizzani V (2010) Climatologia e variabilità interannuale della neve sull'Appennino Emiliano Romagnolo. Quaderno Tecnico ARPA-SIMC n. 19.

De Luis M, Gričar J, Čufar K, Raventós J (2007) Seasonal dynamics of wood formation in *Pinus halepensis* from dry and semi-arid ecosystems in Spain. IAWA J. 28:389–404.

De Luis M, Novak K, Raventós J, Gricar J, Prislan P, Čufar K (2011) Climate factors promoting intra-annual density fluctuations in Aleppo pine (*Pinus halepensis*) from semiarid sites. Dendrochronologia 29:163–169.

De Micco V, Battipaglia G, Cherubini P, Aronne G (2014) Comparing methods to analyse anatomical features of tree rings with and without intra-annual density fluctuations (IADFs). Dendrochronologia 32(1):1-6.

Esper J, Schneider L, Smerdon JE, Schöne BR, Büntgen U (2015) Signals and memory in tree-ring width and density data. Dendrochronologia 35:62–70.

Fritts HC (2001) Tree rings and climate. The Blackburn Press, Caldwell, NJ.

Hamann A, Wang T, Spittlehouse DL, Murdock TQ (2013) A comprehensive, high-resolution database of historical and projected climate surfaces for western North America. Bulletin of the American Meteorological Society 94:1307–1309.

Holmes RL (1983) Computer-assisted quality control in tree-ring dating and measurement. Tree Ring Bulletin 43:69-78.

Jolly WM, Dobbertin M, Zimmermann NE, Reichstein M (2005) Divergent vegetation growth responses to the 2003 heat wave in the Swiss Alps. Geophysical Research Letters 32:L18409.

Klisz M, Koprowski M, Ukalska J, Nabais C (2016) Does the genotype have a significant effect on the formation of intra-annual density fluctuations? A case study using Larix decidua from northern Poland. Front. Plant Sci. 7.

306 Luterbacher J, Dietrich D, Xoplaki E, Grosjean M, Wanner H (2004) European seasonal and annual temperature
307 variability, trends, and extremes since 1500, Science 303(5663):1499–1503.

308 Masiokas M, Villalba R (2004) Climatic significance of intra-annual bands in the wood of *Nothofagus pumilio* in
309 southern Patagonia. Trees 18:696–704.

310 Novak K, Saz-Sánchez MA, Čufar K, Raventós J, De Luis M (2013) Age, climate and intra- annual density fluctuations
311 in *Pinus halepensis* in Spain. IAWA Journal 34:459–474

312 Olano JM, Eugenio M, Carcia-Cervigon AI, Folch M, Rozas V (2012) Quantitative tracheid anatomy reveals a complex
313 environmental control of wood structure in continental Mediterranean climate. International Journal of Plant Sciences
314 173:137-149.

315 Osborn TJ, Briffa KR, Jones PD (1997) Adjusting variance for sample-size in tree-ring chronologies and other regional
316 mean time series. Dendrochronologia 15:1–10.

317 Piermattei A, Crivellaro A, Carrer M, Urbinati C (2015) The "blue ring": anatomy and formation hypothesis of a new
318 tree-ring anomaly in conifers. Trees 29(2): 613-620.

319 Piermattei A, Garbarino M, Urbinati C (2014) Structural attributes, tree-ring growth and climate sensitivity of *Pinus*
320 *nigra* Arn. at high altitude: common patterns of a possible treeline shift in the central Apennines (Italy).
321 Dendrochronologia 32:210–219.

322 Piermattei A, Lingua E, Urbinati C, Garbarino M (2016) *Pinus nigra* anthropogenic treelines in the central Apennines
323 show common pattern of tree recruitment. Eur. J. For. Res. 135:1119–1130.

324 Rigling A, Waldner PO, Forster T, Bräker OU, Pouttu A (2001) Ecological interpretation of tree-ring width and intra-
325 annual density fluctuations in *Pinus sylvestris* on dry sites in the central Alps and Siberia. Can. J. For. Res. 31:18–31.

326 Rigling A, Bräker O, Schneiter G, Schweingruber FH (2002) Intra-annual tree- ring parameters indicating differences in
327 drought stress of *Pinus sylvestris* forests within the Erico-Pinion in the Valais (Switzerland). Plant Ecol. 163(1):105–
328 121.

329 Rivas-Martinez and Rivas-Saenz (2009) Worldwide bioclimatic classification system, 1996–2015. Phytosociological
330 Research Center, Spain. http://www.globalbioclimatics.org

331 Rozas V, Garcia-Gonzalez I, Zas R (2011) Climatic control of intra-annual wood density fluctuations of *Pinus pinaster*
332 in NW Spain. Trees 25:443-453.

Sheppard PR (2010) Dendroclimatology: extracting climate from trees. Wiley Interdiscip. Rev. Clim. Change 1:343–352.

Vieira J, Campelo F, Nabais C (2010) Intra-annual density fluctuations of *Pinus pinaster* are a record of climatic changes in the western Mediterranean region. Can J For Res 40:1567–1575.

Vieira J, Campelo F, Nabais C (2009) Age-dependent responses of tree-ring growth and intra-annual density fluctuations of *Pinus pinaster* to Mediterranean climate. Trees 23:257–265.

Vieira J, Carvalho A, Campelo F (2018) Xylogenesis in the early life stages of maritime pine. Forest Ecology and Management 428. doi: 10.1016/j.foreco.2018.04.037.

Vieira J, Nabais C, Rossi S, Carvalho A, Freitas H, Campelo F (2017) Rain exclusion affects cambial activity in adult maritime pines. Agricultural and Forest Meteorology 237-238:303–310.

Vitali A, Camarero, JJ, Garbarino M, Piermattei A, Urbinati C (2017) Deconstructing human-shaped treelines: Microsite topography and distance to seed source control *Pinus nigra* colonization of treeless areas in the Italian Apennines. Forest Ecology and Management 406:37–45.

Wigley TML, Briffa KR, Jones PD (1984) On the average value of correlated time series, with applications in dendroclimatology and hydrometeorology. J. Clim. Appl. Meteorol. 23:201–213.

Wimmer R, Strumia G, Holawe F (2000) Use of false rings in Austrian pine to reconstruct early growing season precipitation. Can. J. For. Res. 30:1691–1697.

Zalloni E, De Luis M, Campelo F, Novak K, De Micco V, Filippo A, Vieira J, Nabais C, Rozas V, Battipaglia G (2016) Climatic signals from intra-annual density fluctuations frequency in Mediterranean Pines at a regional scale. Front. Plant Sci. 7:1–11.

Tables

Table 1. Main features of the three study sites: VET (Mt. Vettore); SFR (Mt. San Franco); OCR (Mt. Ocre).

	VET	*SFR*	*OCR*
Pine forest upper limit altitude (m a.s.l.)	1600	1500	1350
Altitude range of pioneer pines encroachment (m a.s.l.)	1610 - 2050	1695 - 1930	1635 - 1915
Slope aspect	S-SE	SW-W	N-NE
Slope steepness (%)	35.8	31.7	33.3

Table 2. Main features of the sampled trees at the three study sites. The standard deviation in brackets. PIP, pioneer pines; PLP, planted pines.

PIP	*VET*	*SFR*	*OCR*
No. trees	29	27	24
Mean collar diameter (cm)	18.5 (± 7.8)	16 (± 4.4)	15 (± 5.6)
Mean tree height (cm)	345 (± 178)	274 (± 99)	252 (± 111.6)
Mean cambial age (at collar)	24 (± 5.3)	23 (± 6.2)	24 (± 5.9)

PLP	*VET*	*SFR*	*OCR*
No. trees	19	18	17
Mean DBH (cm)	37.3 (± 3.1)	30.7 (±5.7)	24.7 (± 4.1)
Mean height (m)	11.8 (± 1.1)	11.3 (± 2.1)	20.2 (± 3.2)
Mean cambial age (at DBH)	53 (± 8.2)	43 (± 3)	49 (± 1.9)

Table 3. Summary of the tree-ring chronologies statistics for planted (*PLP*) and pioneer (*PIP*) pines. Range of max, min and mean tree-ring width by tree for the entire length of each series and for the common interval 1984-2008, standard deviation (SD), mean sensitivity (MS), first-order autocorrelation (AC1), interseries correlation (Rbar) and Expressed population signals (EPS). Rbar and EPS were calculated on detrended series for the common interval 1984-2008.

Sites	*Start*	*End*	*Mean TRW (mm)*	*Min TRW (mm)*	*Max TRW (mm)*	*Max TRW (mm) CI 1984-2008*	*SD*	*MS*	*AC1*	*Rbar*	*EPS*
VET PLP	1951	2013	3.00	0.35-2.02	4.47-9.0	2.17-5.78	± 1.534	0.211	0.833	0.412	0.737
VET PIP	1973	2008	2.43	0.12-3.22	1.79-7.28	1.48-7.28	± 0.929	0.286	0.536	0.307	0.639
SFR PLP	1967	2011	2.96	0.36-1.5	4.30-8.17	1.52-6.72	± 1.431	0.223	0.794	0.581	0.847
SFR PIP	1978	2011	2.51	0.09-1.78	1.25-6.57	1.2-6.57	± 1.142	0.353	0.453	0.408	0.674
OCR PLP	1962	2012	2.71	0.21-1.09	6.58-10.6	1.19-4.69	± 1.910	0.252	0.857	0.592	0.813
OCR PIP	1971	2012	1.99	0.11-2.28	1.63-7.52	1.63-7.52	± 0.895	0.364	0.447	0.612	0.863

Table 4. Years with the highest IADFs frequency (stabilized IADFs frequency > 2.5 standard deviation) in each site and considering all planted (PLP) and pioneer (PIP) pines.

Planted			Pioneer			All PLP	All PIP
VET	**SFR**	**OCR**	**VET**	**SFR**	**OCR**		
1965		1965	1987			1973	2000
1971			1996			1974	2001
1973	1973	1973			1997	1977	2003
1974	1974	1974		1998		1983	
		1975		2000	2000	1988	
1977	1977	1977			2001		
	1978		2003	2003	2003		
	1983	1983	2005				
1987					2006		
	1988						

Table 5. Frequency of IADFs latewood type (L and L+ and LL+), in pioneer (PIP) and planted (PLP) pines. The analysis time intervals are for the common interval 1984–2008, and for the entire timespans (in brackets).

Sites	*PLP (L, L+ and LL+)*	*PIP (L, L+ and LL+)*
Entire time span		
VET	20.2 % (1951-2013)	32.8 % (1973-2008)
SFR	40.1 % (1967-2011)	36.5 % (1978-2011)
OCR	30 % (1962-2012)	26.6 % (1984-2012)
Common interval (1984-2008)		
VET	14.3 %	32 %
SFR	34 %	40.3 %
OCR	20%	28.7 %

386 **Figures**

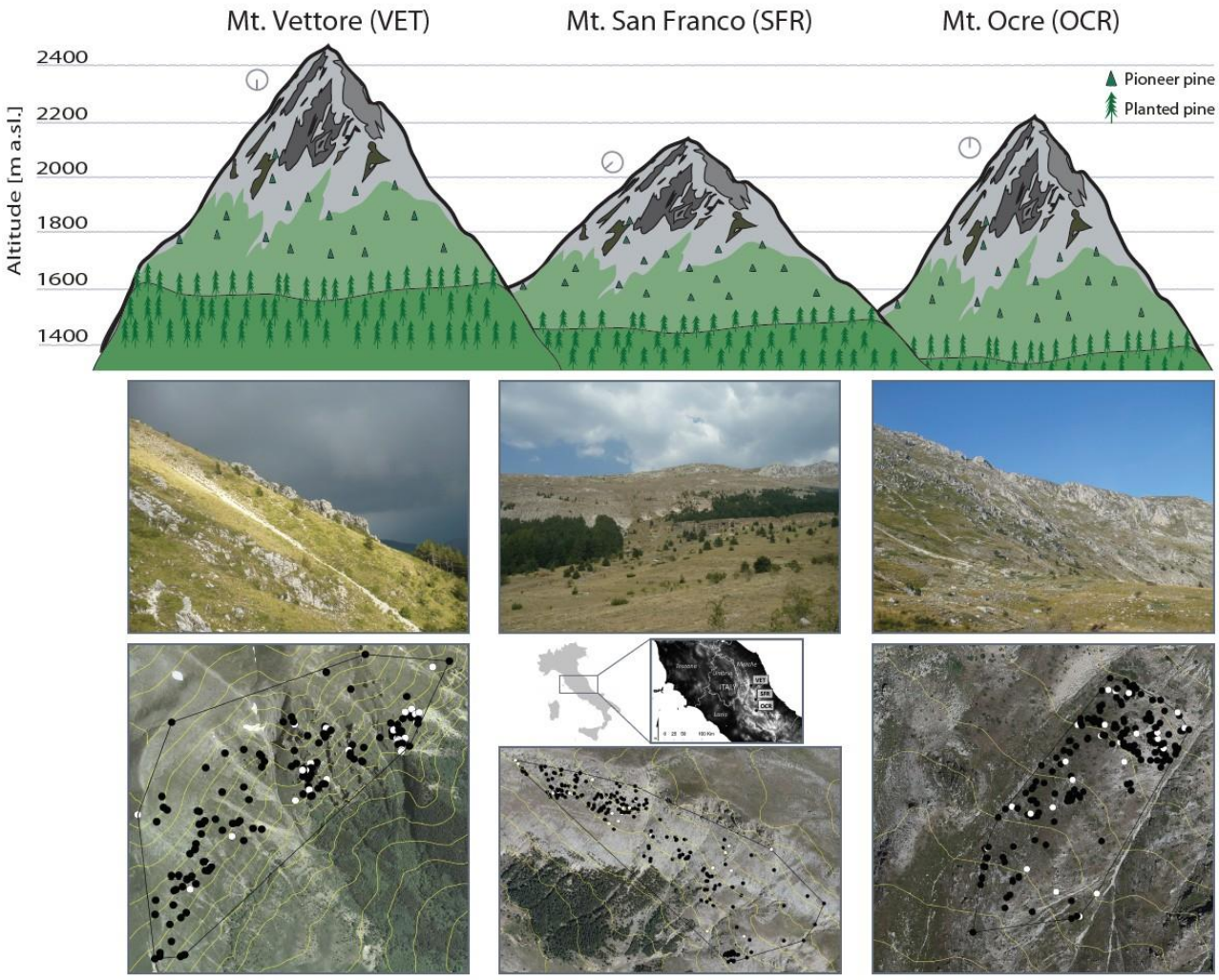

387

388 Figure 1. Representation of the three study sites in the central Apennines (Italy): Mt. Vettore (VET), Mt. San Franco
389 (SFR) and Mt. Ocre (OCR). For each site, from top to bottom: an elevation and aspect layout, an overview picture, and
390 the sampled area with all the mapped trees imposed on the 2010 orthophoto. In the orthophoto there are elevation
391 contours, black dots (all pioneer pines sampled above the forest limit), white dots (pioneer pines analysed for this
392 study). The orientation of the orthophoto is considering the forest limit in the bottom and the peak of the mountain in
393 the top.

394

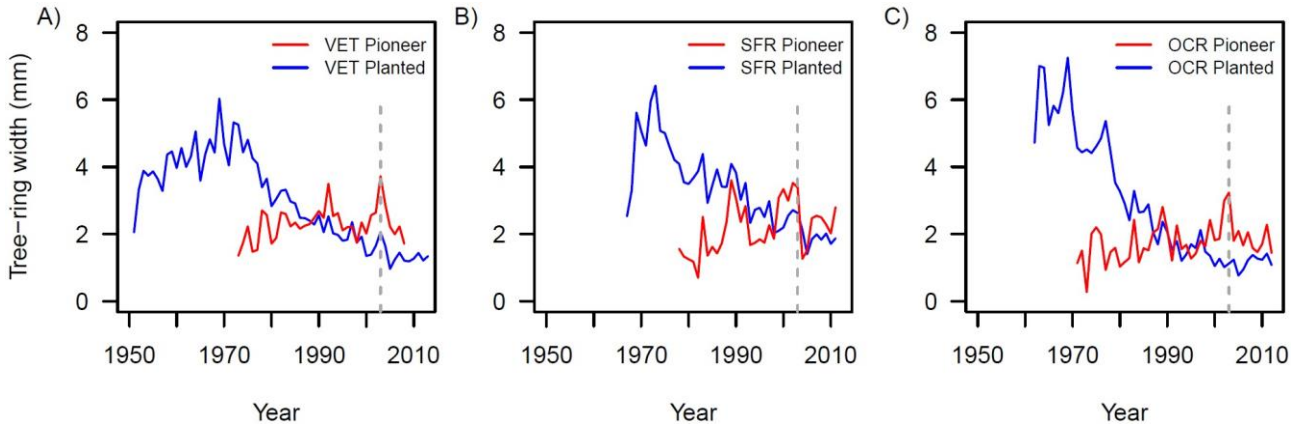

395

396 Figure 2. Tree-ring width chronologies of pioneer (blue) and planted (red) pines at **A)** VET, **B)** SFR, and **C)** OCR sites.

397 The grey dashed line highlights the year 2003, a pointer year with the widest tree ring for pioneer pines.

398

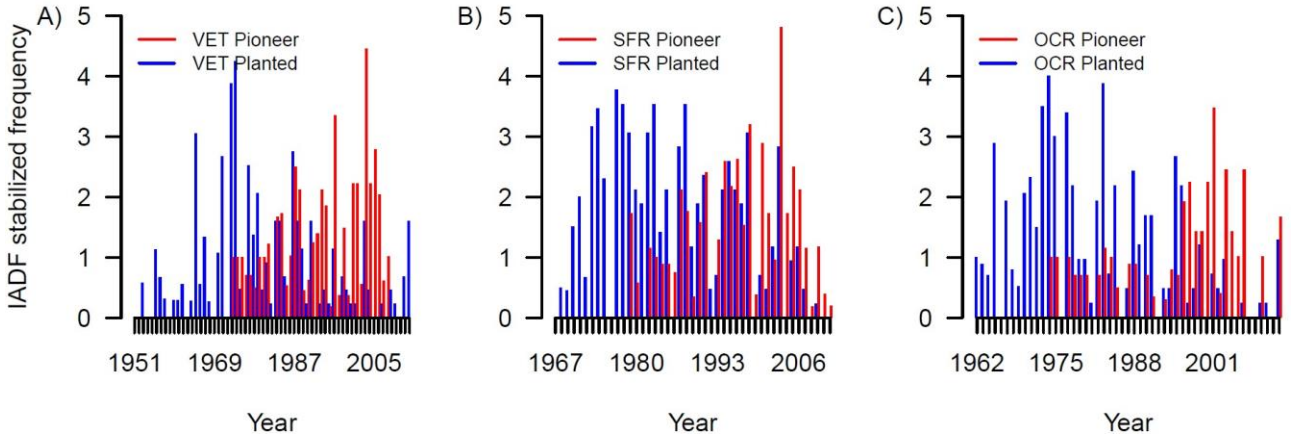

399

400 Figure 3. Stabilized IADFs frequency of pioneer (red) and planted (blue) trees, at **A)** VET, **B)** SFR, and **C)** OCR sites.

401

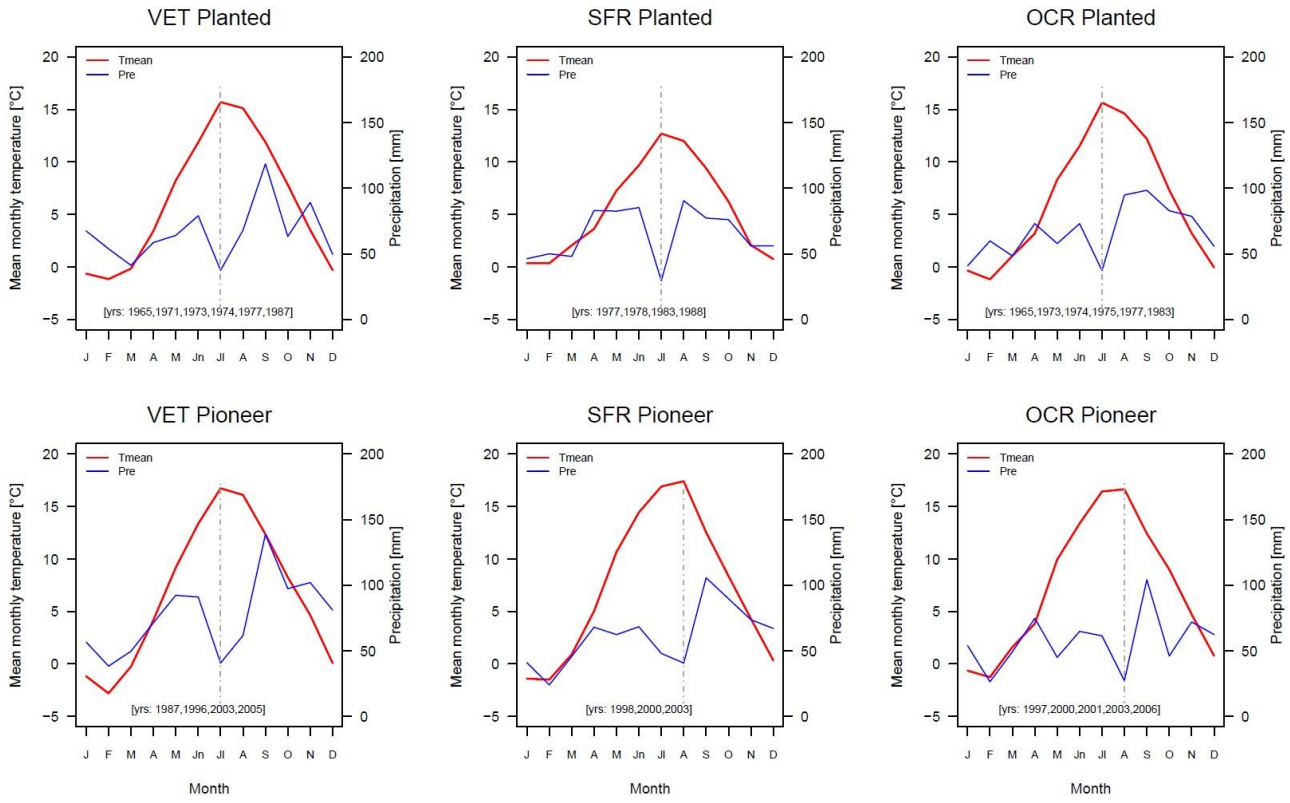

402

403 Figure 4. Trend of mean monthly temperature (red) and mean monthly precipitation (blue) for the years with highest

404 IADFs frequencies (frequency > 2.5 standard deviation), for planted and pioneer pines.

405

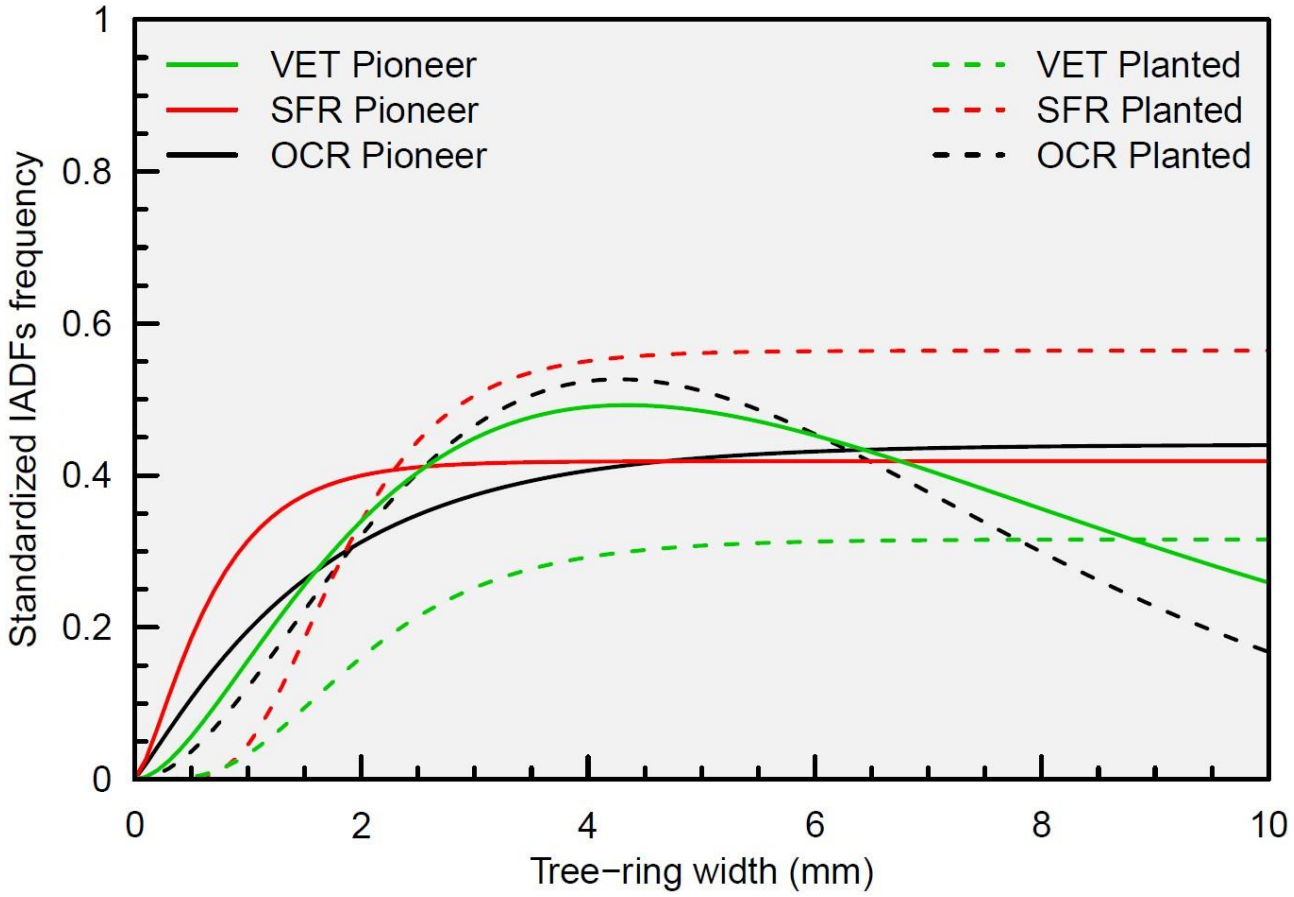

406

407 Figure 5. Standardized IADFs frequency curves as function of tree-ring width under the Chapman and the Weibull

408 functions.

409

410

411

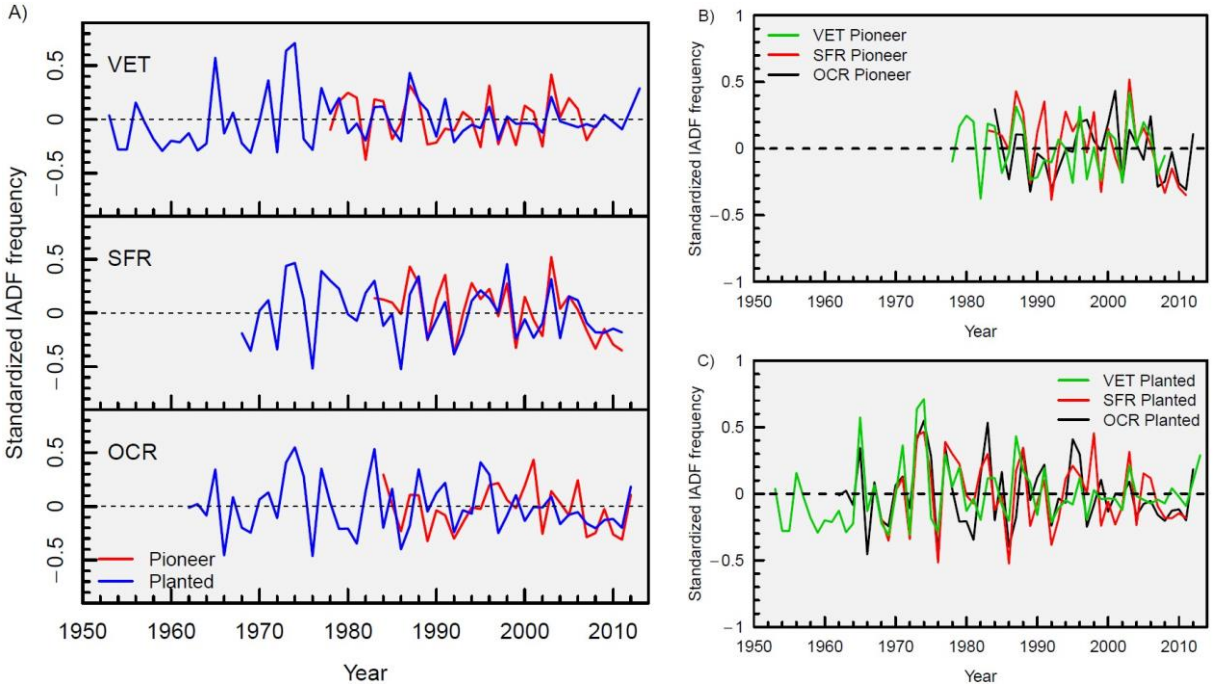

Figure 6. Standardized IADFs chronologies (standardization with removal of age and tree-ring width effect). **A)** A comparison of pioneer and planted pines, **B)** all pioneer pines, and **C)** all planted pines.

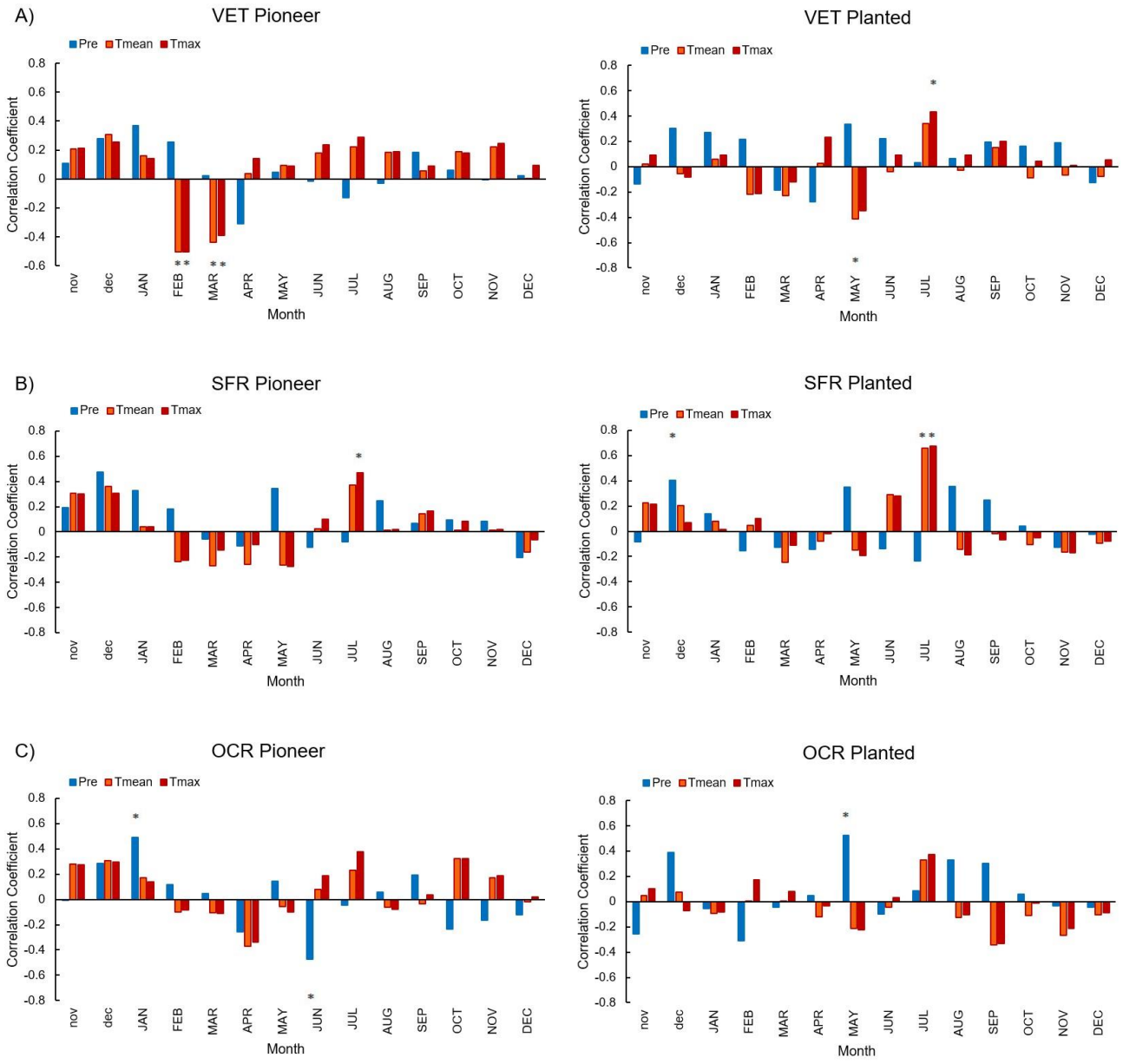

Figure 7. Climate correlation between standardized IADFs chronologies and precipitation (blue), Tmean (orange) and Tmax (red) for the common period 1984-2008 in pioneer and planted pines at **A)** VET, **B)** SFR and **C)** OCR sites. Asterisk (*) indicates significant correlation ($P < 0.05$).